Molecular Biology of the Cell
Vol. 9, 2125–2144, August 1998

Efficient Trafficking of TGN38 from the Endosome to the trans-Golgi Network Requires a Free Hydroxyl Group at Position 331 in the Cytosolic Domain

Elizabeth P. Roquemore and George Banting*

Department of Biochemistry, University of Bristol School of Medicine, University Walk, Bristol BS8 1TD, England

Submitted July 3, 1997; Accepted May 4, 1998
Monitoring Editor: Ira Mellman

TGN38 is one of the few known resident integral membrane proteins of the trans-Golgi network (TGN). Since it cycles constitutively between the TGN and the plasma membrane, TGN38 is ideally suited as a model protein for the identification of post-Golgi trafficking motifs. Several studies, employing chimeric constructs to detect such motifs within the cytosolic domain of TGN38, have identified the sequence ^{333}YQRL^{336} as an autonomous signal capable of localizing reporter proteins to the TGN. In addition, one group has found that an upstream serine residue, S331, may also play a role in TGN38 localization. However, the nature and degree of participation of S331 in the localization of TGN38 remain uncertain, and the effect has been studied in chimeric constructs only. Here we investigate the role of S331 in the context of full-length TGN38. Mutations that abolish the hydroxyl moiety at position 331 (A, D, and E) lead to missorting of endocytosed TGN38 to the lysosome. Conversely, mutation of S331 to T has little effect on the endocytic trafficking of TGN38. Together, these findings indicate that the S331 hydroxyl group has a direct or indirect effect on the ability of the cytosolic tail of TGN38 to interact with trafficking and/or sorting machinery at the level of the early endosome. In addition, mutation of S331 to either A or D results in increased levels of TGN38 at the cell surface. The results confirm that S331 plays a critical role in the intracellular trafficking of TGN38 and further reveal that TGN38 undergoes a signal-mediated trafficking step at the level of the endosome.

INTRODUCTION

One of the first proteins to be identified as a resident of the trans-Golgi network (TGN) was TGN38 (Luzio *et al.*, 1990), a heavily glycosylated type I integral membrane protein with a 33-amino acid cytosolic domain. TGN38 cycles constitutively between the TGN and the plasma membrane, but at steady state is localized predominantly to the TGN (for review see Banting and Ponnambalam, 1997). Since TGN38 moves through both the endocytic and exocytic pathways during cycling, it has been used as a model protein to identify post-Golgi localization motifs.

The majority of investigations aimed at identifying such sequences have involved the use of chimeric constructs composed of various domains of TGN38 fused to heterologous reporter proteins normally localized to the cell surface. Several such studies have identified a tetrapeptide tyrosine-based sequence, ^{333}YQRL^{336}, located in the cytosolic domain of TGN38, that is capable of localizing reporter proteins to the TGN (Bos *et al.*, 1993; Humphrey *et al.*, 1993; Wong and Hong, 1993) This sequence also conforms to the YXXΦ motif (where Φ is any bulky hydrophobic amino acid) characteristic of proteins that are internalized from the cell surface via clathrin-mediated endocytosis (for reviews see Trowbridge *et al.*, 1993; Marks *et al.*, 1997). One investigation employing chimeric constructs has further implicated an upstream serine residue, S331, as important for localization of reporter proteins to the TGN (Wong and Hong, 1993). However, two previous studies failed to identify S331 as

* Corresponding author.

important for TGN localization but found, instead, that YQRL alone was necessary and sufficient for localization of chimeric constructs to the TGN (Bos *et al.*, 1993; Humphrey *et al.*, 1993). Thus, although SXYQRL is widely cited as the minimum TGN localization motif within TGN38, evidence for the importance of S331 remains in dispute and has never been tested in the context of full-length TGN38.

Other conflicting reports concerning the putative SXYQRL localization motif have emerged through the use of chimeric studies. For example, when transferrin receptor was used as the reporter protein, the SDYQRL sequence was unable to localize the chimeric protein to the TGN, but instead directed it to an altered recycling compartment (Johnson *et al.*, 1996). Furthermore, YQRL alone was sufficient to confer this localization. In another study, the SDYQRL motif was not sufficient to divert delivery of the reporter protein lgp120 from lysosomes to the TGN (Reaves *et al.*, 1998). The results of these investigations imply that information obtained through the study of chimeric molecules may vary according to the reporter protein chosen. Thus, although chimeric constructs are a powerful tool for identification of possible post-Golgi localization motifs, it is becoming increasingly apparent that a full understanding of the mechanism by which those motifs regulate the complex itinerary of proteins such as TGN38 can only be obtained by examining potential trafficking motifs in the context of the full-length protein from which they are derived.

Like other YXXΦ motifs, the YQRL sequence of TGN38 is believed to interact in vivo with one or more adaptor protein (AP) complexes, which mediate vesicle formation at the cell surface, the TGN, and possibly the endosome (Marks *et al.*, 1997, review). Using a yeast two-hybrid system, Ohno et al. (1995, 1996) found that the sequence YQRL within the cytosolic domain of TGN38 is capable of interacting with the μ1, μ2, and μ3 (p47A) subunits (of the AP1, AP2, and AP3 adaptor complexes, respectively), and that mutation of the upstream Ser residue (S331) to Ala had little or no effect on these interactions. In contrast, two-hybrid binding studies using the entire cytosolic domain of TGN38 (Stephens *et al.*, 1997 and our unpublished observations) demonstrate that mutation of S331 to either A or D disrupts interactions between the μ2 subunit and the cytosolic domain of TGN38. These conflicting data further underscore the need for careful reexamination of the role of S331, preferably in a whole-cell system in which S331 is mutated in the context of full-length TGN38.

While most tyrosine-based sorting signals are capable of mediating delivery from the plasma membrane to the endosomes, there is now growing evidence that some YXXΦ motifs, including YQRL, are involved in downstream intracellular sorting events as well (for reviews see Sandoval and Bakke, 1994; Marks *et al.*, 1997). The molecular basis by which cytosolic trafficking machinery is able to distinguish between the wide array of YXXΦ motifs, thereby effecting delivery of integral membrane proteins to their correct intracellular destinations, is not yet clear. Thus, it is possible that additional trafficking motifs may be required in conjunction with the YXXΦ motif to allow intracellular sorting steps to occur. For example, the trafficking of a number of integral membrane proteins containing cytosolic YXXΦ motifs appears to be modulated by transient phosphorylation of serine/threonine residues elsewhere within their cytosolic domains. Examples include the polymeric immunoglobulin (Ig) receptor (Okamoto *et al.*, 1994; Song *et al.*, 1994; Mostov, 1995), the TGN-resident endoprotease furin (Jones *et al.*, 1995; Takahashi *et al.*, 1995; Dittie *et al.*, 1997), and both the cation-independent and cation-dependent mannose-6-phosphate receptors (Kornfeld, 1992; Korner *et al.*, 1994; Mauxion *et al.*, 1996). All of these proteins have been found to contain, in addition to the YXXΦ motif, a cytosolic S/T-containing casein kinase II consensus sequence. Interestingly, dephosphorylation of the casein kinase II consensus site within the cytosolic tail of furin has been correlated with exit of furin from an endocytic recycling pool and entry into a TGN-directed pathway (Jones *et al.*, 1995). In addition, the cation-dependent mannose-6-phosphate receptor contains yet another type of signal sequence that prevents it from being delivered to the lysosomal compartment (Rohrer *et al.*, 1995; Schweizer *et al.*, 1996). Since no additional sorting signals other than the YXXΦ motif have yet been identified within the cytosolic domain of TGN38, we and others have proposed that transient phosphorylation of residues in the vicinity of the Y residue might modulate the interaction of sorting machinery with the YQRL sequence of TGN38 (Wong and Hong, 1993; ZehaviFeferman *et al.*, 1995; Banting and Ponnambalam, 1997). In support of this hypothesis, in vitro radioisotope labeling experiments indicate that all of the S/T residues in the cytosolic domain of TGN38 can be phosphorylated either by PKC or PKA (ZehaviFeferman *et al.*, 1995).

To address the role of S331 in the trafficking of TGN38, and to examine the possible effects of constitutive phosphorylation at S331, we have generated stably transfected cell lines expressing either wild-type TGN38 or TGN38 in which S331 has been mutated to either A or D. The latter mutation was chosen as a means by which we might potentially mimic constitutive phosphorylation (Casanova *et al.*, 1990; Thorsness and Koshland, 1987). In addition, we have used transiently transfected cells to examine the effects of mutating S331 to T or E. The results demonstrate that S331 plays a role in the sorting of endocytosed TGN38 from the endosome. Mutations that abolish the free hydroxyl moiety at position 331 (A, D, or E) result

in missorting or delayed exit of TGN38 from the endosome, while mutation of S331 to T has little effect, suggesting that accessibility of a free serine hydroxyl moiety at position 331 is essential for correct endocytic trafficking of TGN38 between the endosome and the TGN.

MATERIALS AND METHODS

Materials

Unless otherwise specified, all reagents were purchased from Sigma Chemical (Dorset, England). Brefeldin A was diluted to a 5 mg/ml stock solution with methanol and stored at −20°C. LY294002, an inhibitor of phosphoinositol-3-kinase, was purchased from Calbiochem-Novabiochem UK (Nottingham, England), and stored at −20°C as a 50 mM stock solution in DMSO. Cycloheximide was stored at −20°C as a 15 mg/ml stock in methanol. Glycl-phenylalanine 2-naphthylamide (GPN) was stored at −20°C as a 200 mM stock in DMSO. Texas Red-conjugated transferrin was purchased from Molecular Probes Europe (Cambridge, England) and stored at 4°C as 5 mg/ml stock in PBS. Restriction enzymes for recombinant DNA procedures were purchased from Boehringer Mannheim UK (East Sussex, England).

Recombinant DNA Procedures

All constructs were cloned into the mammalian expression vector, ΔpMEP, using standard cloning procedures (Sambrook *et al.*, 1989). ΔpMEP contains a multiple cloning site downstream of the human metallothionein II promoter, which can be induced by heavy metals. It also carries the Hygromycin B resistance gene for selection in eukaryotic cells. ΔpMEP was created from pMEP-4 (Invitrogen BV, Leek, The Netherlands) by removing the OriP and EBNA-1 genes responsible for episomal maintenance of the plasmid. The resulting 5570-base pair (bp) vector must be integrated into the eukaryotic host genome to undergo replication.

Rat TGN38 cDNA was amplified in the vector pUEX1 (Luzio *et al.*, 1990) and excised by digestion with *Bam*HI. To create TGN38-ΔpMEP, full-length rat TGN38 cDNA was inserted into the *Bam*HI site of the ΔpMEP multiple cloning site. The Ser at position 331 of TGN38 was mutated by PCR using a 5′-primer (5′-GGTACCAGACTACAGGATGCAGTTCCTGG-3′), which created an *Asp* 718 I restriction site at the 5′-end of the TGN38 cDNA, in conjunction with one of the following 3′-primers: 5′-AAGCTTTAGGTTCAAACGTTGGTAGTCAGCGGCCTTTGG-3′; 5′-AAGCTTTAGGTTCAAACGTTGGTAGTCATCGGCCTTTGG-3′; 5′-AAGCTTTAGGTTCAAACGTTGGTAGTCTTCGGCCTTTGG-3′; or 5′-AAGCTTTAGGTTCAAACGTTGGTAGTCGGTGGCCTTTGG-3′, which converted the Ser at position 331 to A, D, E, or T, respectively, and preserved a *Hin*dIII site at the 3′-end of the insert. PCR was performed for 20 cycles according to the manufacturer's suggestions using the Expand High Fidelity thermostable DNA polymerase mixture (Boehringer Mannheim, Mannheim, Germany). The PCR products were then subcloned into pGEM-T (Promega UK, Southampton, England), excised by digestion with *Asp*718 I and *Hin*dIII, and ligated with the 5.6-kilobase (kb) fragment created by digestion of TGN38-ΔpMEP with *Asp*718 I and *Hin*dIII. Dideoxy chain termination sequencing demonstrated that only the desired mutations had been introduced into the cytosolic tail of TGN38 and that the stop codon had been retained.

Antibodies

The following antibodies were used: *2F7.1*, a mouse monoclonal antibody raised against the extreme 13 amino-terminal amino acids of mature rat TGN38 (Horn and Banting, 1994 [hybridoma supernatant], and Affinity Bioreagents, Golden, CO [murine ascites]); *1918*, a rabbit polyclonal antibody raised against the extreme 13 amino-terminal amino acids of mature rat TGN38; *shG29*, a sheep polyclonal antibody raised against a TGN41/β-galactosidase fusion protein, and subsequently shown to recognize epitopes common to both TGN38 and its homologue TGN41; *RbG29*, a rabbit polyclonal antibody raised against a TGN41/β-galactosidase fusion protein. The polyclonal antibodies listed above were generated and characterized by Wilde *et al.* (1992). To identify the monkey orthologue (species homologue) of TGN38, we used the rabbit polyclonal antibody *P12*, which was generated against human TGN46 (Prescott *et al.*, 1997) and which cross-reacts with the endogenous monkey orthologue present in Cos-7 cells, but not with rat TGN38.

Cell Culture and Transfections

Cos-7 cells (derived from African green monkey kidney fibroblasts) were maintained at 37°C and 5% carbon dioxide in DMEM containing 10% heat-inactivated FBS, 100 μg/ml streptomycin, and 100 U/ml penicillin.

ΔpMEP containing TGN38 or one of its mutant isoforms was transfected into Cos-7 cells by electroporation or lipofection. For electroporation, 5×10^6 log-phase Cos-7 cells were washed three times in ice-cold PBS and resuspended in 300 μl ice-cold buffer containing 20 mM HEPES, pH 7.0, 137 mM sodium chloride, 5 mM potassium chloride, 0.7 mM disodium orthophosphate, 250 mM sucrose, and 20 μg linearized purified plasmid DNA. The cell suspension was then electroporated at room temperature in a 0.4-cm cuvette at 300 V, 500 μF. After a recovery period of 10 min at room temperature, the electroporated cells were transferred to a 75-cm^2 tissue culture flask containing DMEM/10% FBS. Forty-eight hours after electroporation, selection was begun by the addition of Hygromycin B (Boehringer Mannheim) at a final concentration of 400 μg/ml. Stable clones were selected 2–3 wk later and maintained in DMEM/10% FBS containing 200 μg/ml Hygromycin B.

For lipofection, 5×10^6 log-phase Cos-7 cells were washed three times in ice-cold PBS and preincubated for 10 min with serum-free DMEM. Purified plasmid DNA was then mixed with Transfectam Reagent (Promega, Madison, WI) and applied to the cells according to the manufacturer's instructions. After a 16-h incubation period, the lipofection reagent was replaced with DMEM/10% FBS. Selection with Hygromycin B (Boehringer Mannheim) at a final concentration of 400 μg/ml was begun 48 h after transfection. Stable clones were maintained in DMEM/10% FBS containing 200 μg/ml Hygromycin B.

Immunofluorescence and Confocal Laser Scanning Microscopy

Indirect immunofluorescence microscopy was performed as previously described (Reaves and Banting, 1992) on stably transfected cells grown on sterilized glass coverslips to a confluence of 50–80%. Cells were stimulated for 18 h with cadmium chloride (at concentrations specified in the text) to induce expression from the metallothionein promoter, treated with pharmacological agents as necessary, rinsed twice with PBS, and fixed by one of the two following methods: 1) to assess whether or not TGN38 was at the cell surface, cells were fixed by incubating at room temperature in PBS containing 3% paraformaldehyde, 1 μM calcium chloride, 1 μM magnesium chloride. After paraformaldehyde fixation, cells were incubated for 3 min at room temperature in the absence or presence of 0.1% Triton X-100, which permeabilizes the cells; 2) for all other experiments, cells were incubated at −20°C for 5 min in methanol, which simultaneously fixes and permeabilizes the cells.

After fixation, the cells were rinsed once in PBS and blocked for 15 min in PBS containing 1% BSA (fraction V, Sigma Chemical). After addition of the appropriate primary and secondary antibodies, cells were rinsed three times in PBS and mounted on glass slides with Mowiol solution (10% Mowiol 4–88 [Calbiochem-Novabiochem, San Diego, CA], 25% glycerol, 0.1 M Tris, pH 8.5, 2.5% 1,4-

diazabicyclo[2.2.2]octane [Sigma Chemical]). Cells were examined with a Leica TCS-NT confocal laser scanning unit equipped with a Kr/Ar laser and attached to a Leica DM RBE upright epifluorescence microscope. All images were collected with a 63× oil immersion objective lens, and processed with Leica software for 2D image analysis.

Carbohydrate Analysis

Glycosidase reactions and lectin affinity precipitation (our unpublished results) were performed on TGN38 that had been immunoprecipitated from Cos-7 cells expressing the wild-type protein using shG29 polyclonal antibody as described above. For glycosidase reactions, protein was eluted from the beads by boiling for 10 min in 100 μl reaction buffer containing 1% NP-40, 15 mM EDTA, 0.1 M sodium cacodylate, pH 6.0. After cooling on ice, eluted proteins were incubated at 4°C for 18 h in the absence (control) or presence of one or more of the following enzymes: *N*-glycanase (200 mU, Genzyme, Boston, MA); sialidase from *Arthrobacter ureafasciens* (50 mU, Boehringer Mannheim); *O*-glycosidase from *Diplococcal pneumoniae* (2.5 mU, Boehringer Mannheim). After glycosidase treatment, samples were boiled in sample buffer and analyzed by 8% SDS-PAGE and immunoblotting as described above.

For lectin affinity precipitation, protein was eluted from immunoprecipitation beads by boiling in 0.5% SDS, 0.1 M sodium cacodylate, pH 6.0. After cooling on ice, samples were diluted to 1 ml in PBS containing 0.5% BSA, 2.5% NP-40, and 5 mM calcium chloride and incubated with 20 μl wheat germ agglutinin-conjugated Sepharose for 2 h at 4°C. After affinity precipitation, beads were washed three times with RIPA buffer and analyzed by 8% SDS-PAGE.

Internalization of Monoclonal Antibody to TGN38

Internalization of TGN38 was monitored by following uptake of the monoclonal antibody to TGN38, 2F7.1. Cells were grown on glass coverslips to 50–80% confluence. 2F7.1 ascites (Affinity Bioreagents, Golden, CO) was then added to the tissue culture medium at a dilution of 1:400, and the cells were incubated at 37°C for up to 2 h. To identify late endosomal compartments, the wortmannin analogue LY294002 was added to a final concentration of 50 μM during the final 30 min of incubation.

To examine the effect of GPN, cells were preincubated for 10 min in the presence of 200 μM GPN to induce a lysosomal block. Subsequently, 2F7.1 ascites was added to the culture medium at a dilution of 1:400 in the continued presence of GPN, and uptake was allowed to proceed for 25 min. Concomitant with antibody uptake, Texas Red-conjugated transferrin was added to the tissue culture medium (final concentration, 10 μg/ml) to label endocytic compartments. After incubation, cells were rinsed twice with PBS, fixed with methanol, and processed for immunofluorescence microscopy as described above.

Biotinylation Experiments

For surface biotinylation, cells and all solutions were precooled on ice. After rinsing twice with PBS and once with PBS containing 0.7 mM calcium chloride/0.25 mM magnesium sulfate (PBS^{++}), cells were incubated on ice for 30 min in 40 mM sodium bicarbonate, pH 8.6, containing 1.5 mg/ml EZ-link sulfo-NHS-SS-Biotin (Pierce & Warriner, Chester, England), a membrane-impermeable disulfide-linked biotinylation reagent. After biotinylation, cells were rinsed twice with PBS^{++}, and biotinylation was stopped by the addition of 50 mM glycine in PBS^{++}. The cells were then lysed, and biotinylated material was affinity isolated with streptavidin-agarose as described below. Unbiotinylated TGN38 was immunoprecipitated from the remaining lysate using a mixture of 2F7.1 monoclonal and shG29 polyclonal antibodies by the method described below.

Treatment with Cycloheximide and Lysosomal Inhibitors

Cells were treated with 15 μg/ml cycloheximide for 0–3 h at 37°C to inhibit protein synthesis. TGN38 isoforms were precipitated from cell lysates with a sheep polyclonal antibody to TGN38 (shG29) and immunoblotted with a rabbit polyclonal antibody to TGN38 (1918). Protein levels were compared by densitometry, and results are expressed as percentage of total initial TGN38 or mutant isoform remaining at each time point (n = 3). To examine the effect of lysosomal inhibitors on the turnover rate of S331D, cells were preincubated in the presence of LPEM (20 mM methionine methyl ester, 100 μg/ml leupeptin, 100 μg/ml pepstatin A, and 100 μg/ml E64) for 2 h before the addition of cycloheximide and throughout the 3-h time course.

Cell Lysis and Affinity Precipitation

Cells were lysed on ice by scraping into 750 μl ice-cold 10 mM Tris, 50 mM sodium chloride, 0.05% NP-40, 0.1% SDS, 0.5% sodium deoxycholate, pH 8 (RIPA) containing protease inhibitors (1 mM PMSF, 1 μg/ml leupeptin, 2 μg/ml antipain, 10 μg/ml benzamidine, 1 μg/ml chymostatin, 1 μg/ml pepstatin A, 10 U/ml aprotinin, 4 mM EDTA). Lysates were then sonicated briefly on ice and centrifuged at 4°C for 20 min at 10,000 × *g*.

For biotinylation experiments, biotinylated proteins were affinity isolated from the clarified supernatant using an estimated 10-fold excess of streptavidin-agarose. In other experiments, proteins were immunoprecipitated with antibodies (specified in the figure legends and described above) that had been prebound to GammaBind G Sepharose (Pharmacia Biotech, Uppsala, Sweden). Streptavidin- or antibody-conjugated beads were incubated with the clarified cell lysates for 2–4 h at 4°C, pelleted by brief centrifugation, and washed four times with ice-cold RIPA. Proteins were eluted from the beads by boiling in sample buffer (10% glycerol, 2% SDS, 1% β-mercaptoethanol, 0.1% bromophenol blue, 50 mM Tris, pH 6.8) and resolved by SDS-PAGE on 8% polyacrylamide gels.

Immunoblotting

Polyacrylamide gels were electroblotted to polyvinylidene difluoride (PVDF) membranes (New England Nuclear Research Products, Boston, MA) at 200 mA for 2 h in buffer containing 25 mM Tris, 192 mM glycine, 20% methanol. The membranes were then blocked for 1 h in TBS containing 0.1% Tween 20 (TBST) and 10% nonfat dried milk. Primary antibodies were diluted in TBST and incubated with the membranes for 2 h at room temperature with constant mixing. After rinsing the blots three times in TBST, HRP-conjugated secondary antibodies (Sigma Chemical) were added in TBST at a dilution of 1:10,000. Blots were incubated for a further hour, rinsed three times in TBST, and developed by ECL using ECL detection reagents (Amersham International, Buckinghamshire, England) according to the manufacturer's instructions.

Comparison of Protein Expression Levels

To compare protein expression levels in the transfected cell lines, equal numbers of cells were lysed for each sample, and total TGN38 was immunoprecipitated with a molar excess of shG29 as described above. Immunoprecipitated proteins were resolved by 8% SDS-PAGE and electroblotted to PVDF membranes. TGN38 variants were detected with 1918 polyclonal antibody followed by HRP-conjugated anti-rabbit Ig and ECL as described above. Levels of proteins in different lanes on the same immunoblot were compared by density profile analysis performed on a Macintosh Quadra 650 computer using the public domain NIH Image program (developed at the US National Institutes of Health and available on the Internet at http://rsb.info.nih.gov/nih-image/). The technique of immunoprecipitating TGN38 before immunoblotting was employed to improve the detection of TGN38 by allowing the concentration of

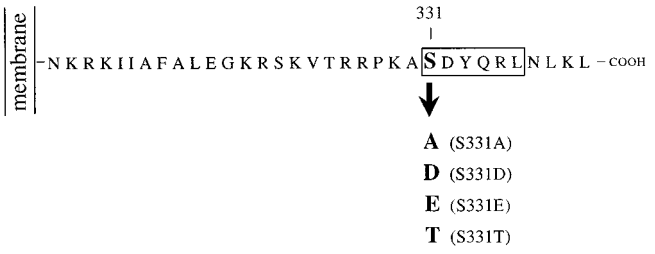

Figure 1. Schematic representation of the TGN38 constructs generated by PCR mutagenesis. Schematic representation of the TGN38 variants described in MATERIALS AND METHODS. Only the cytosolic domains are depicted in the diagram.

TGN38 from relatively large populations of cells. Similar results were obtained by immunoblotting whole-cell lysates directly.

Molecular Modeling

Molecular modeling of wild-type and mutant forms of the cytosolic domain of TGN38 was performed using InsightII 95.0.6 (MSI/Biosym, San Diego, CA). Based on the results of previous two-dimensional nuclear magnetic resonance analysis (Wilde *et al.*, 1994), which indicated that the SDYQRL motif of TGN38 lies within an α-helix, the peptides shown in Figure 11 were built as regular α-helices. Side-chain torsions were manipulated as described below.

RESULTS

Characterization of Cos-7 Cell Lines Stably Expressing TGN38, S331A, and S331D

To examine the effect of S331 mutations on the intracellular trafficking of TGN38, we generated stably transfected Cos-7 cell lines expressing TGN38, S331A, and S331D (Figure 1). Indirect immunofluorescence confocal microscopy of the stable cell lines shows that both the S331 mutants and wild-type TGN38 are similarly localized to a juxtanuclear compartment characteristic of the Golgi/TGN (Figure 2, A, C, and E). The cells shown in Figure 2 have been induced to express comparable levels of protein (see below). Under these conditions, the fluorescence intensities of the TGN38 isoforms are also comparable. In addition, both wild-type and mutant TGN38 proteins colocalize with the endogenous monkey orthologue (Figure 2, B, D, and F).

It has been shown previously that gross overexpression of TGN38 can lead to apparent mislocalization of the protein (Reaves and Banting, 1994). It has also been shown that the intracellular machinery responsible for the appropriate localization of TGN38 is saturable (Luzio *et al.*, 1990). We therefore maintained that, to make valid comparisons between the various forms of TGN38 expressed in Cos-7 cells, it was necessary to ensure that the recombinant proteins were expressed at similar levels in the transfected cells, and that these levels were comparable to those of endogenous TGN38 in normal rat kidney cells. The expression of TGN38 variants in each cell line was adjusted to similar levels by titrating the amount of cadmium chloride added to the tissue culture medium. Concentrations of up to 20 μM cadmium chloride have been shown to have no effect on the gross morphology or viability of Cos-7 cells (Reaves and Banting, 1994). Densitometric analysis of immunoblots similar to the one shown in Figure 3A was performed to compare the level of expression of TGN38 constructs in each of the transfected cell lines. The results of two such experiments are summarized in Table 1. Within each data set presented in the table, it is apparent that the total expression levels of wild-type TGN38, S331A, and S331D are comparable both to each other and to the levels of endogenous wild-type TGN38 in untransfected normal rat kidney cells. On the basis of these results, the indicated concentrations of cadmium chloride were used for all subsequent experiments, unless otherwise indicated.

Immunoblot analysis of TGN38 isolated from the transfected cell lines identifies a pattern of bands that is similar for all three constructs expressed (Figure 3A). Wild-type TGN38, S331A, and S331D all migrate as a doublet of approximately 104/111 kDa. This agrees with the reported molecular weights for fully glycosylated forms of TGN38 (Yuan *et al.*, 1987; Luzio *et al.*, 1990; Jones *et al.*, 1993). Also present in all three cell lines is an additional immunoreactive doublet at approximately 69/71 kDa. The relative mobility of the 69/71 kDa doublet changes with respect to the length of the carboxy-terminal tail, migrating with a higher M_r when the tail is lengthened, and with a lower M_r when the tail is shortened (our unpublished observations), indicating that it consists of lower M_r forms of TGN38. To further confirm that this lower M_r doublet consists of biosynthetic precursors of mature fully glycosylated TGN38, we treated normal rat kidney cells (expressing wild-type TGN38) with 15 μg/ml cycloheximide. After 3 h of cycloheximide treatment, the lower M_r doublet of TGN38 is no longer apparent (Figure 3B), as would be expected for a biosynthetic intermediate. Cycloheximide treatment led to disappearance of the lower M_r doublet in all of the stable transfectants. In addition, the lower M_r doublet was never detected at the cell surface by biotinylation (see below), further confirming that it consists of biosynthetic precursors to mature TGN38. Carbohydrate analysis revealed that the immature TGN38 precursors observed in Figure 3A contain nonsialylated N-linked carbohydrates, but have not yet acquired the O-linked carbohydrates found in the mature forms, consistent with a *cis*/medial Golgi localization (our unpublished results). It is noteworthy that the relative abundance of the immature forms of wild-type TGN38 is 15% of the total population of TGN38 molecules, whereas in cells expressing S331A and S331D mutants the relative abundance of immature forms

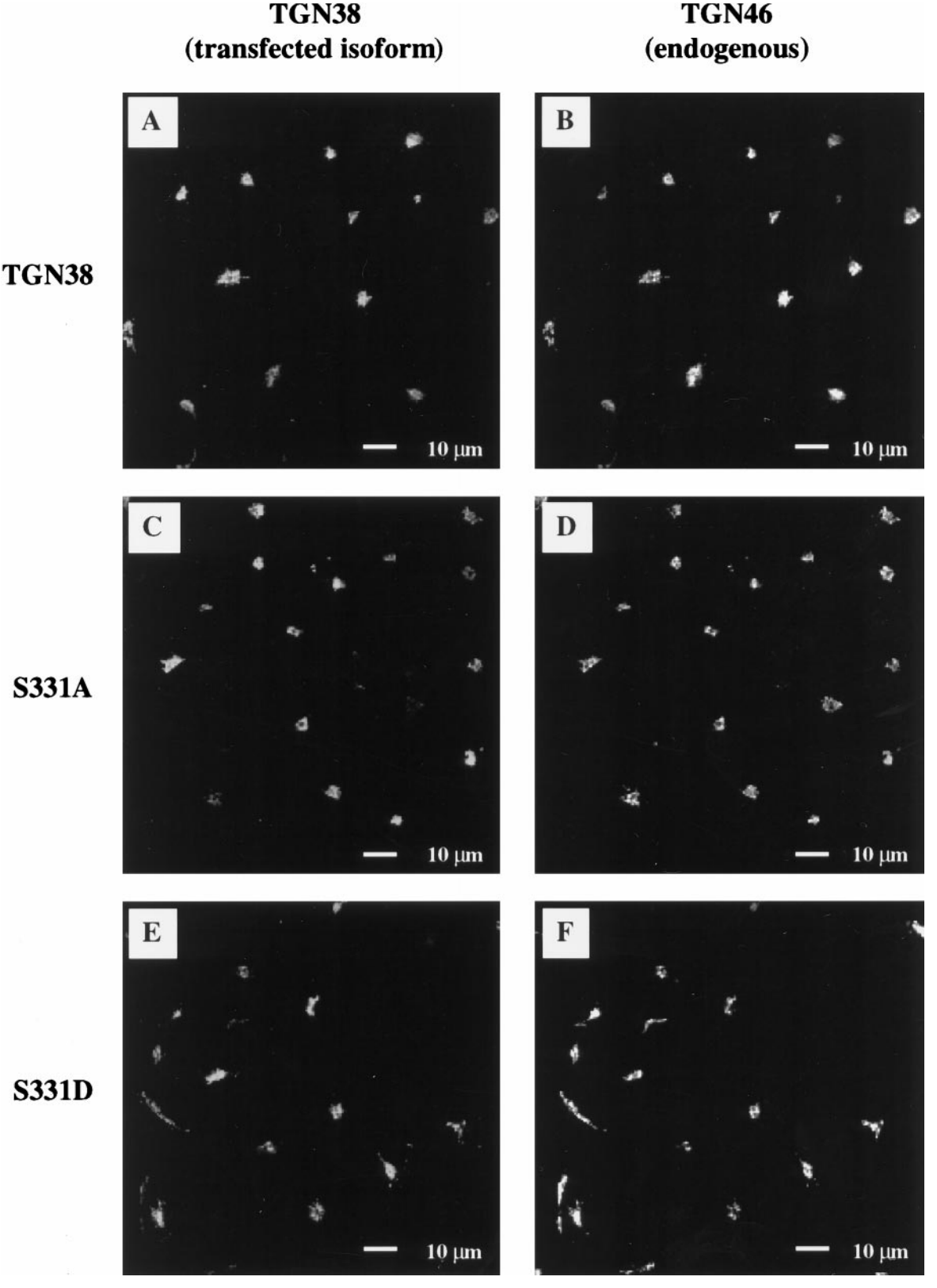
TGN38
(transfected isoform)
TGN46
(endogenous)
TGN38
S331A
S331D
A
B
C
D
E
F
10 μm
10 μm
10 μm
10 μm
10 μm
10 μm

Figure 2.

rises to 38 and 42%, respectively (Figure 3C). As discussed below, this may reflect subtle differences in the overall steady-state distribution of S331A and S331D due to their enhanced degradation.

As shown in Figure 2, wild-type TGN38, S331A, and S331D all localize to a juxtanuclear compartment resembling the Golgi/TGN. Because the Golgi and the TGN cannot be distinguished by indirect immunofluorescence alone, we treated the cells with Brefeldin A, a fungal metabolite that has differential effects on the Golgi cisternae and the TGN (Lippincott-Schwartz *et al.*, 1990, 1991; Reaves and Banting, 1992). In response to Brefeldin A, proteins in the Golgi cisternae reportedly redistribute to the endoplasmic reticulum, while those in the TGN redistribute to the microtubule-organizing center. As shown in Figure 4A, after treatment for 1 h with 5 μg/ml Brefeldin A, wild-type TGN38 is located predominantly in the region of the microtubule-organizing center, confirming that the majority of TGN38 is localized to the TGN at steady state. Similarly, S331A and S331D are also localized to the microtubule-organizing center after Brefeldin A treatment (Figure 4, B and C). However, as would be expected from the relative increase in Golgi-localized immature forms of S331A and S331D observed by immunoblot analysis (Figure 3C), a subfraction of S331A and S331D molecules redistributes to the endoplasmic reticulum in response to Brefeldin A (Figure 4, B and C).

In the Absence of Protein Synthesis, Degradation of S331A and S331D Is Elevated Compared with Degradation of Wild-Type TGN38

One possible explanation for our observation that the ratio of immature to mature forms is increased in cells expressing the S331A and S331D mutants is that mature forms of S331A and S331D are degraded more rapidly than mature forms of wild-type TGN38. To assess the relative degradation rates of wild-type TGN38, S331A, and S331D, we followed the disappearance of TGN38 and the S331 mutants as a function

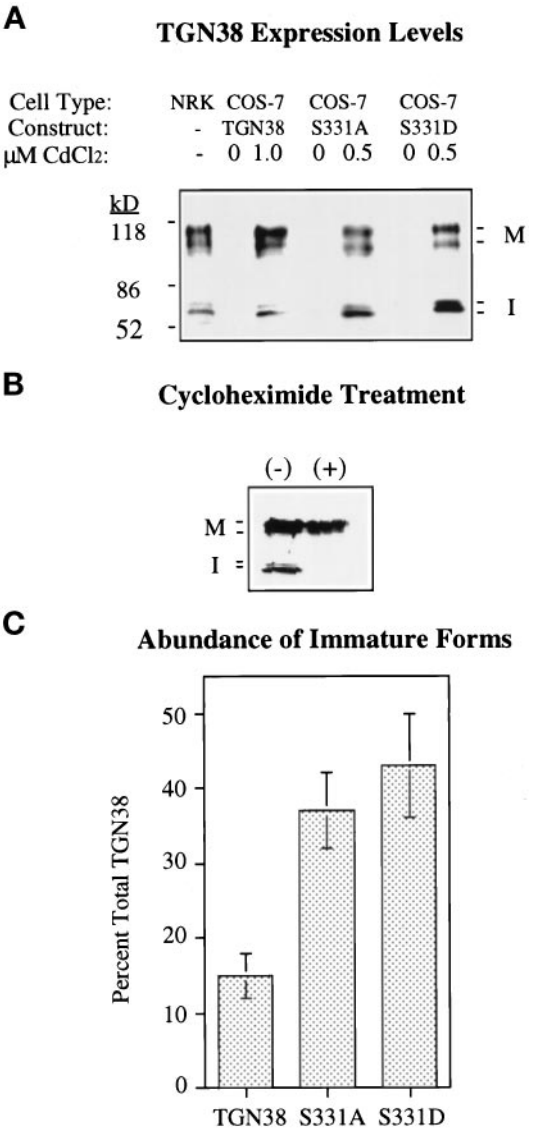

Figure 3. Immunoblot analysis of TGN38 variants expressed in transfected cell lines. (A) Induction of expression. TGN38 constructs were stably expressed in Cos-7 African green monkey kidney fibroblasts and induced to comparable expression levels from the human metallothionein IIa promoter by the addition of empirically determined concentrations of cadmium chloride ($CdCl_2$) to the tissue culture medium. Equal numbers of cells were lysed for each sample, and total TGN38 was immunoprecipitated with an excess of sheep polyclonal anti-TGN38 (shG29). Immunoprecipitated proteins were detected by immunoblot with a rabbit polyclonal antibody to TGN38 (1918) followed by HRP-conjugated anti-rabbit Ig and ECL. M, mature forms; I, immature forms. (B) Cycloheximide treatment to identify biosynthetic intermediates. Normal rat kidney cells were incubated in the absence or presence of 15 μg/ml cycloheximide for 3 h. Endogenous TGN38 was then immunoprecipitated and immunoblotted as described above; a similar effect of cycloheximide on the immature doublet was observed for all of the transfected cell lines. (C) Comparison of the relative abundance of immature forms of TGN38. The percentage of total TGN38 variant present as an immature lower M_r doublet was determined for each stably transfected cell line by density profile analysis of immunoblots prepared as described above. ($\pm$SD, n = 3).

Figure 2 (facing page). Indirect immunofluorescence microscopy of TGN38 variants expressed in Cos-7 cells. TGN38 constructs were stably expressed in Cos-7 African green monkey kidney fibroblasts and induced to comparable expression levels from the human metallothionein IIa promoter by the addition of empirically determined concentrations of cadmium chloride to the tissue culture medium. Cells expressing wild-type TGN38 (A and B), S331A (C and D), and S331D (E and F) were dual labeled with a mixture of monoclonal antibody against rat TGN38 (2F7.1) and polyclonal antibody recognizing the endogenous monkey orthologue of TGN38 (P12). Antibody to TGN38 was visualized by incubation with FITC-conjugated anti-mouse Ig as secondary antibody (panels A, C, and E). Antibody to the endogenous monkey orthologue was visualized by incubation with Texas Red-conjugated anti-rabbit Ig as secondary antibody (panels B, D, and F).

Table 1 Comparison of protein expression levels in cells expressing TGN38, S331A, and S331D

			DATA SET 1		DATA SET 2	
Cell type	Transfected construct	$CdCl_2$ (μM)	Total peak area[a]	Deviation[b]	Total peak area[a]	Deviation[b]
NRK	None	None	1633	1.00	3697	1.04
Cos-7	Wild-type TGN38	1.0	1675	1.02	3748	1.05
Cos-7	S331A	0.5	1680	1.03	3667	1.03
Cos-7	S331D	0.5	1665	1.02	3560	1.00

For each data set, equal numbers of cells were stimulated with the indicated concentrations of cadmium chloride, lysed, immunoprecipitated, and immunoblotted as described in MATERIALS AND METHODS. Levels of protein in different lanes on the same immunoblot were compared by density profile analysis.

[a]Total peak area is defined as the sum of the peak areas generated by mature and immature forms detected in each cell line.

[b]Deviation was calculated by normalizing total peak areas within each data set to the lowest value in that set.

of time in the absence of protein synthesis. After treatment of transfected cell lines with cycloheximide for 0–3 h, levels of the immunoprecipitated proteins were quantified by densitometric scanning of immunoblots and expressed as percent total TGN38 isolated at time zero. As indicated in Figure 5, both S331A and S331D are indeed degraded more rapidly than wild-type TGN38. After 3 h of incubation in the presence of cycloheximide, levels of S331A and S331D are decreased by 80%, while wild-type TGN38 is decreased only 31% over the total detectable at time zero. In contrast, when a mixture of lysosomal inhibitors (LPEM) was added to cells expressing S331D 2 h before addition of cycloheximide and throughout the 3-h time course, degradation of S331D was significantly inhibited (Figure 5, D+LPEM). Thus, the reduced half-lives of S331A and S331D can be attributed to degradation in a prelysosomal or lysosomal compartment.

Mutation of the Cytosolic Tail at S331 to Either A or D Elevates the Level of TGN38 at the Cell Surface

Having characterized the stably transfected cell lines and established that steady-state levels of the protein were comparable, we were in a position to examine the endocytic trafficking of wild-type TGN38, S331A, and S331D. Since previous in vitro binding studies had suggested that mutations at S331 might decrease the affinity of the cytosolic domain of TGN38 for clathrin-mediated endocytosis machinery (Stephens *et al.*, 1997), we first examined the cell surface distribution of the TGN38 variants, initially by indirect immunofluorescence of unpermeabilized cells. Cells were fixed with paraformaldehyde, treated in the absence or presence of detergent, and probed with monoclonal antibody 2F7.1. As shown in Figure 6, C and E, both S331A and S331D are apparent at the cell surface of unpermeabilized cells. In contrast, wild-type TGN38 is not detectable at the cell surface using this technique (Figure 6A). In the parallel control cells, detergent permeabilization confirmed that all three cell lines were indeed expressing the transfected constructs and that the majority of the protein expressed was localized to the TGN in each case (Figure 6, B, D, and F).

Cell surface biotinylation was performed to compare the relative amount of TGN38, S331D, or S331A at the cell surface. Biotinylated proteins were affinity isolated from whole-cell lysates with streptavidin-conjugated beads. Nonbiotinylated TGN38 was then immunoprecipitated from the lysates with an excess of TGN38 antibody (shG29). Precipitated proteins were analyzed by immunoblot, using anti-TGN38 polyclonal antibodies (RbG29 and 1918), followed by density profile analysis. Calculation of the percentage of TGN38 variants at the cell surface, as indicated in Figure 7, reveals that 2.9 $\pm$ 0.6% of S331A and 4.0 $\pm$ 0.5% of S331D are present at the cell surface, as compared with only 0.2% of wild-type TGN38. Thus, levels of the S331A and S331D mutants at the cell surface are increased 15- to 20-fold over wild-type TGN38. This marked increase in cell surface levels of S331A and S331D cannot be accounted for by overexpression and the consequent saturation of endocytic machinery, since it has been demonstrated previously that even a 10-fold overexpression of the wild-type protein produces no detectable increase at the cell surface (Reaves and Banting, 1994).

Mutation of S331 to A or D Increases the Flux of TGN38 Through a Lysosomal Pathway

We next compared the ability of cells expressing S331A, S331D, or wild-type TGN38 to endocytose TGN38 and deliver it to the TGN. If, as shown in Figure 5, S331A and S331D are degraded more rapidly than wild-type TGN38, one might expect to find more S331A and S331D routed along a lysosomal rather than a TGN-directed pathway, relative to the wild-type protein. To follow the endocytic routing of

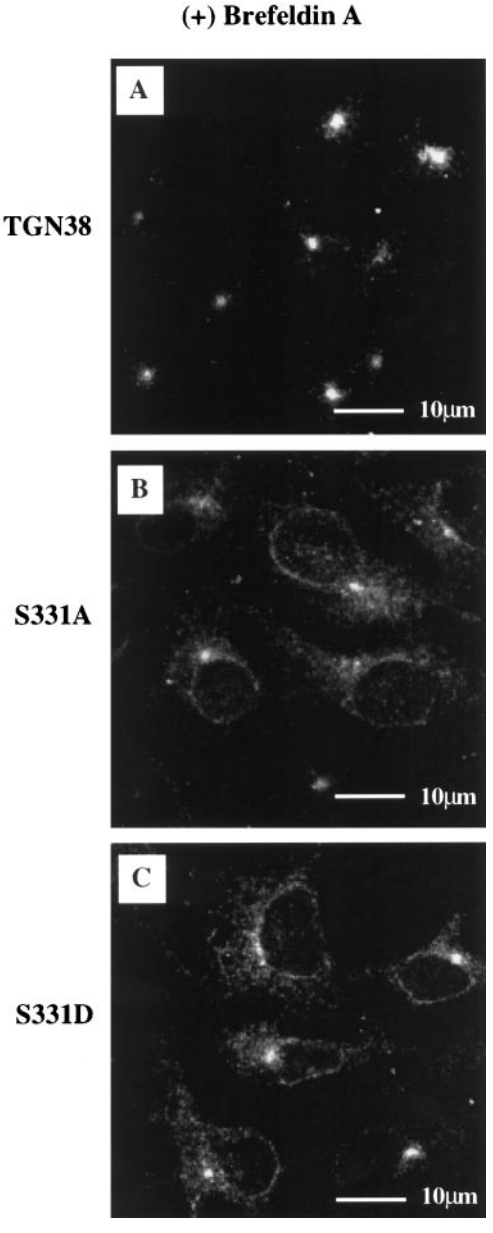

Figure 4. Brefeldin A treatment. Cells were grown on glass coverslips and induced to comparable expression levels by the addition of cadmium chloride in the concentrations indicated in Figure 3A. After treatment with 5 μg/ml Brefeldin A for 1 h at 37°C, cells were fixed and permeabilized with methanol and processed for immunofluorescence by incubation with a monoclonal antibody against TGN38 (2F7.1) followed by FITC-conjugated anti-mouse secondary antibody. (A) Wild-type TGN38; (B) S331A; (C) S331D.

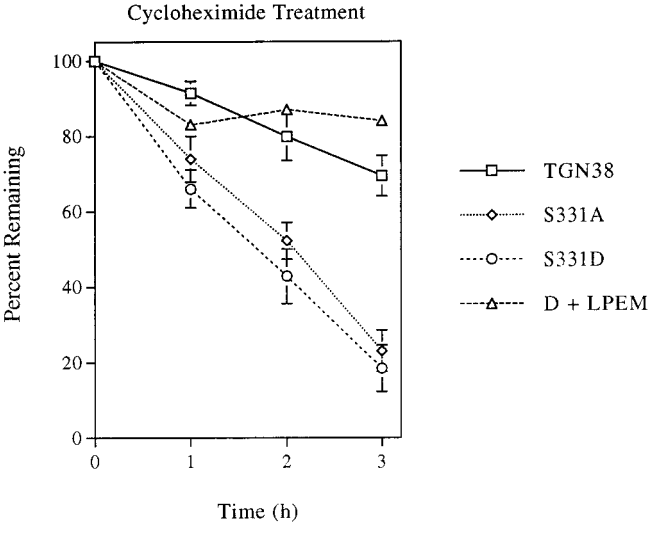

Figure 5. Degradation of TGN38 isoforms. Cells were treated with cycloheximide for 0–3 h at 37°C to inhibit protein synthesis. TGN38 variants were precipitated from cell lysates with a sheep polyclonal antibody to TGN38 (shG29) and immunoblotted with a rabbit polyclonal antibody to TGN38 (1918). Protein levels were compared by densitometry, and results are expressed as percentage of total initial TGN38 variant remaining at each time point (±SD, n = 3). In one experiment, cells expressing S331D were preincubated in the presence of a mixture of lysosomal inhibitors (LPEM) for 2 h before the addition of cycloheximide and throughout the 3-h time course (n = 1).

TGN38, we used the antibody uptake assay previously described by Reaves *et al.* (1993). The monoclonal antibody 2F7.1, which recognizes the extracellular amino terminus of TGN38, was added to the tissue culture medium of cells expressing wild-type TGN38, S331A, or S331D, and endocytosis was allowed to occur for 2 h at 37°C. Cells were then fixed, costained with antibody to endogenous TGN46 to visualize the TGN, and analyzed by indirect immunofluorescence. In cells expressing wild-type TGN38, the extracellularly added monoclonal antibody to TGN38 largely colocalizes with antibody to the endogenous monkey orthologue after 2 h of continuous uptake (Figure 8A; areas where the two antibodies colocalize are pseudocolored yellow). However, even in clonal populations of cells, some degree of variation in the ability to endocytose 2F7.1 is to be expected (our unpublished observations), and may be cell cycle stage dependent. Hence, staining of some cells in the population appear yellow, indicating that they are efficiently endocytosing TGN38, while others appear red, containing mainly endogenous TGN46 and little endocytosed TGN38. Nonetheless, it is clear that, in cells that are actively undergoing 2F7.1 uptake, endocytosed wild-type TGN38 is efficiently delivered to, and retained in, the TGN. In contrast, after 2 h of uptake by cells expressing S331A or S331D (Figure 8, C and E, respectively), the monoclonal antibody is present not only in the TGN, but also in numerous peripheral vesicular structures that contain little if any endogenous monkey orthologue (arrows). Again, not all cells are actively endocytosing the exogenous antibody, but those cells that do take up the antibody show a profusion of

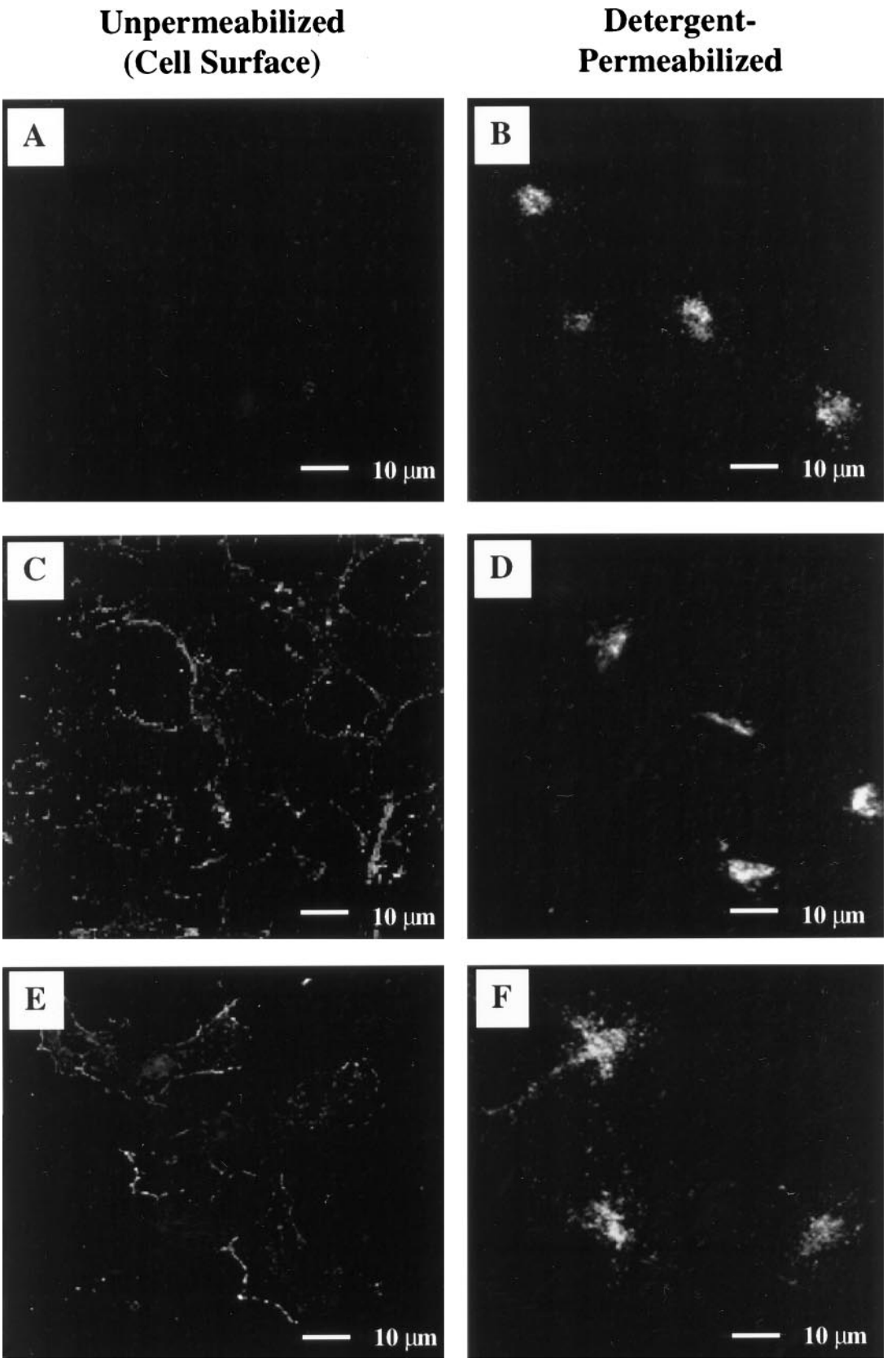
Unpermeabilized
(Cell Surface)
Detergent-
Permeabilized
A
B
C
D
E
F
10 μm
10 μm
10 μm
10 μm
10 μm
10 μm

Figure 6.

peripheral vesicular structures. Thus, while the mutation of S331 to A or D does not prohibit clathrin-mediated endocytosis of TGN38, it does interfere with efficient routing or retrieval of TGN38 to the TGN.

As a means of identifying the peripheral vesicular structures observed in Figure 8 (panels C and E), we examined the effects of two independent pharmacological agents, each reported to have differential effects on various endocytic/lysosomal compartments. The first, LY294002, is believed to block trafficking out of late and recycling endosomes by inhibiting phosphoinositol 3-kinase (PI3K) (Reaves *et al.*, 1996; Shepherd *et al.*, 1996). Reaves *et al.* (1996) observed that treatment with LY294002 markedly altered the morphology of late endosomes (and possibly recycling endosomes), causing them to swell considerably. In contrast, they did not observe swelling of early endosomes (e.g., lucifer yellow-containing endocytic vesicles) in response to LY294002. In fact, PI3K inhibition has been correlated with a decrease in early endosome volume (Clague *et al.*, 1995). Using PI3K inhibitors in conjunction with antibody uptake, Reaves *et al.* (1996) have shown that wild-type TGN38 is routed from the early endosome to the TGN without appearing in LY294002-sensitive late endosomes to any significant degree, while the lysosomal integral membrane protein lgp120, internalized from the cell surface, becomes trapped in the swollen late endosomes. We conducted antibody uptake experiments using concentrations of LY294002 similar to those used by Reaves and co-workers. Cells were allowed to endocytose monoclonal antibody to TGN38 (2F7.1) for 2 h to reveal the distribution of TGN38, S331A, or S331D. During the final 30 min of uptake, swollen vesicles were induced by the addition of 50 μM LY294002 as a means of identifying late and/or recycling endosomes. Fixed cells were costained with antibody to endogenous TGN46 to visualize the TGN. As shown in Figure 8B, and in agreement with the findings of Reaves *et al.* (1996), wild-type TGN38 was not observed in swollen vesicles after LY294002 treatment and therefore does not accumulate in LY294002-sensitive endosomal compartments to any detectable degree. In contrast, structures containing endocytosed 2F7.1 in the S331 mutant cell lines appear swollen after LY294002 treatment (panels D and F, arrowheads). These results suggest that, unlike wild-type TGN38, significant proportions of S331A and S331D traffic through, or are delayed in, late endosomes and/or the recycling compartment after internalization from the cell surface.

In at least one case, PI3K inhibition has been observed to cause swelling of early endosomes as well as late and recycling endosomes (Shpetner *et al.*, 1996). Therefore, to distinguish further between lysosomal and endosomal compartments, we examined the effects of the membrane-permeable dipeptide GPN. GPN is a cathepsin C substrate, which has been used in vitro on mixed vesicle populations to selectively disrupt lysosomes (defined as those vesicles containing acid phosphatases) but not prelysosomal endocytic compartments (Berg *et al.*, 1994). Within the lysosome, GPN is cleaved to a membrane-impermeable

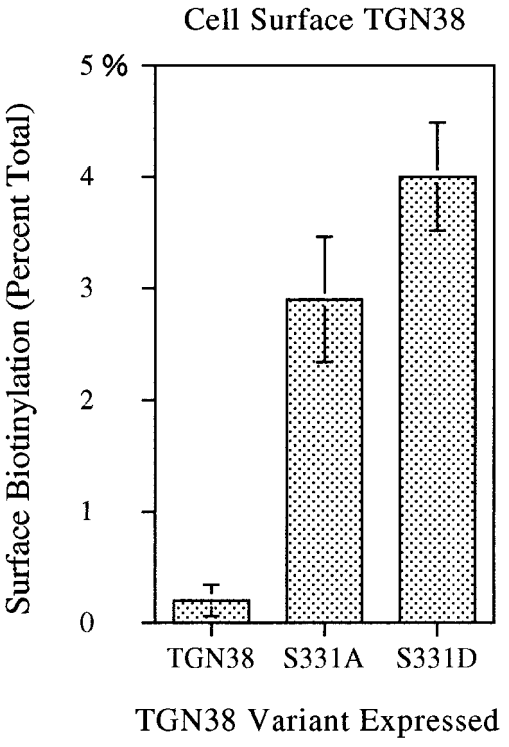

Figure 7. Detection of cell-surface expression of TGN38 variants by surface biotinylation. Cells induced to comparable expression levels were cooled on ice and biotinylated with disulfide-linked biotin for 30 min to label cell surface proteins. Biotinylated proteins were affinity isolated from cell lysates with streptavidin-agarose beads. The remaining TGN38 was immunoprecipitated with a polyclonal antibody to TGN38 (shG29). Affinity- and immuno-precipitated proteins were processed and analyzed by densitometry as described in MATERIALS AND METHODS. Cell surface (biotinylated) TGN38 is expressed as the percentage of total TGN38 (biotinylated plus unbiotinylated) affinity isolated in each case (± SD, n = 3). (In parallel control samples, no endocytosis was observed in cells incubated on ice.)

Figure 6 (facing page). Detection of cell-surface expression of TGN38 variants by indirect immunofluorescence. Cells expressing wild-type TGN38 (A and B), S331A (C and D), or S331D (E and F) were subjected to paraformaldehyde fixation followed by incubation in the absence (A, C, and E), or presence (B, D, and F) of 0.1% Triton X-100 to permeabilize the plasma membrane. TGN38 was detected with a monoclonal antibody to TGN38 (2F7.1) followed by FITC-conjugated anti-mouse Ig. Surface antigen on detergent-permeabilized cells is not visible in these images due to the comparatively bright epifluorescence contributed by staining of intracellular TGN38.

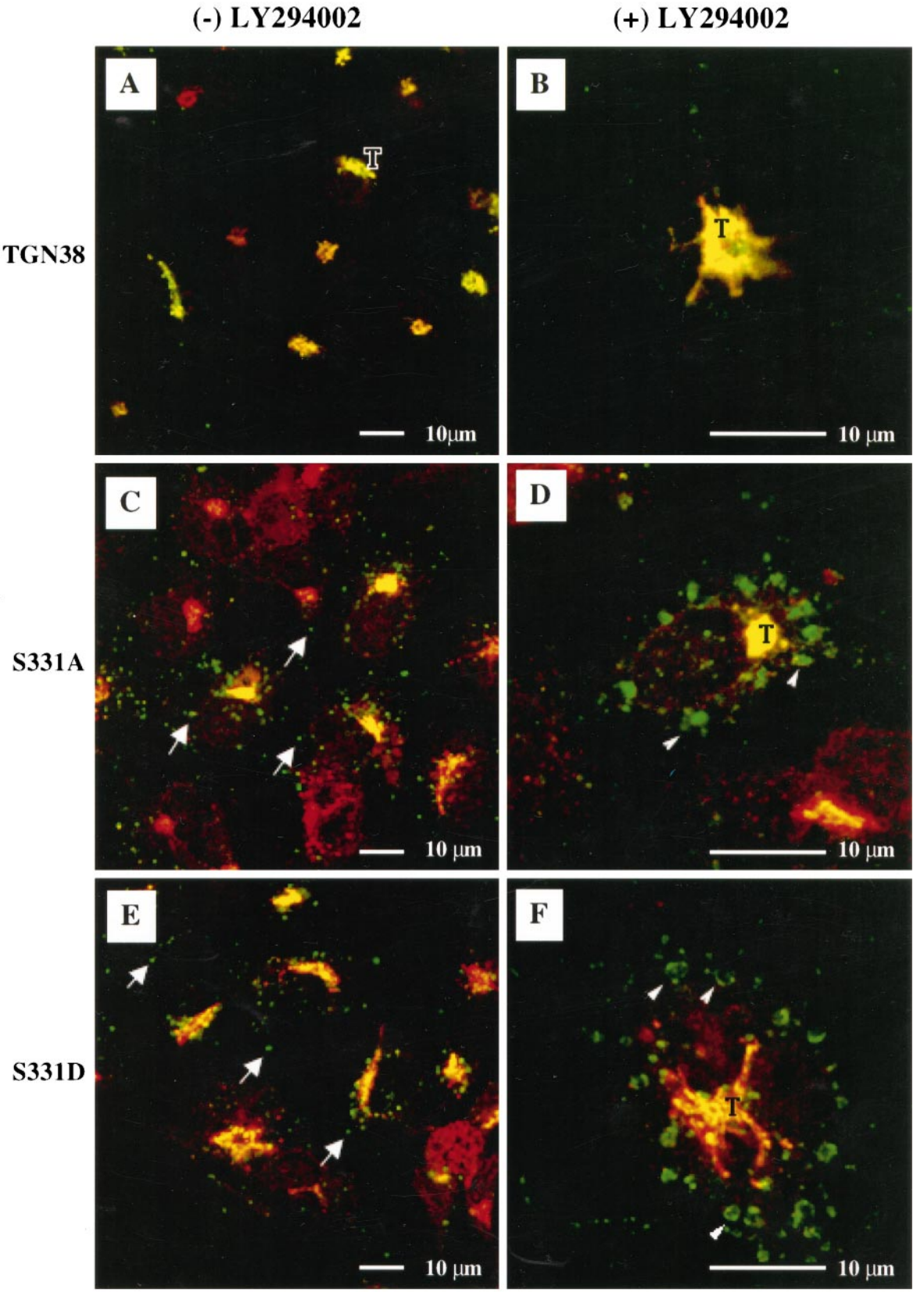

Figure 8.

form by cathepsin C. Accumulation of the cleavage product causes lysosomes to swell and eventually rupture. In this assay, we examined the kinetics of antibody uptake in GPN-treated cells. Cells expressing S331D, S331A, or wild-type TGN38 were pretreated for 10 min with GPN to induce lysosomal swelling. Subsequently, in the continued presence of GPN, monoclonal antibody 2F7.1 was added extracellularly to the cells for increasing amounts of time. Texas Red-conjugated transferrin was added to the culture medium during antibody uptake to label endosomal structures. As shown in Figure 9, in cells expressing the S331A or S331D mutants, endocytosed 2F7.1 was observed in swollen vesicles generated by GPN after 25 min of uptake (Figure 9, B and C), but not at an earlier time point of 20 min (our unpublished observation). The nonswollen, 2F7.1-containing structures also observed (arrows) are likely to be endosomal carrier vesicles. In cells expressing wild-type TGN38, endocytosed antibody was not observed in swollen vesicles during the same 25-min uptake period (Figure 9A). The kinetics of appearance of the S331 mutants in the swollen vesicles suggests that the protein reaches the lysosomal compartment along an endocytic route. Furthermore, we observe little, if any, colocalization of the S331A or S331D with Texas Red-conjugated transferrin, consistent with trafficking through the lysosome rather than the recycling endosome (Figure 9).

Substitution of E at Position 331 Alters the Endocytic Trafficking of TGN38

The substitution of D at position 331 was originally intended to mimic constitutive phosphorylation. The observation that mutation of S331 to either A or D has a similar effect on the endocytic trafficking of TGN38 thus implies that the observed changes in endocytic trafficking of S331A and S331D were not due to the inability to phosphorylate Ser 331, but rather due to the absence, in either construct, of a free hydroxyl group at position 331. However, it was also possible that, in our experimental system, D was not a successful mimic of constitutive phosphorylation. Reports of the use of D as a mimic of constitutive phosphorylation indicate variable degrees of success. Since E has been reported in some cases to be a better mimic of phosphorylation than D (for example, see Kortnenjann *et al.*, 1994), we expressed the S331E mutant (Figure 1) transiently in Cos-7 cells and examined the cells for their ability to endocytose and correctly deliver monoclonal anti-TGN38 antibody (2F7.1) to the TGN. As shown in Figure 10, panel E, S331E mutants were partially routed to a juxtanuclear compartment (asterisk) identified as the TGN by Brefeldin A treatment (our unpublished observation). However, a significant portion of S331E also appeared in peripheral vesicular structures (panel E, arrows) similar to those observed for the S331A and S331D mutants. Upon treatment with LY294002 (Figure 10F), S331E accumulates in swollen late endosomal structures (arrows), consistent with routing along a lysosomal pathway. Thus, S331E, S331D, and S331A appear to be similarly routed along a late endosomal/lysosomal pathway after endocytosis from the cell surface. In a parallel control, transiently transfected wild-type TGN38 did not appear in LY294002-sensitive compartments and was efficiently routed to the TGN (Figure 10, A and B). Even in cells expressing markedly high levels of wild-type TGN38, no swollen compartments were observed in response to LY294002 (our unpublished observation).

The Hydroxyl Group of S331 Is Important for Correct Trafficking of TGN38 at the Level of the Endosome

The simplest explanation for the similar behavior of S331A, S331D, and S331E, with respect to their endocytic trafficking, is that accessibility of the S331 hydroxyl group is important for efficient routing of TGN38 between the endosome and the TGN. Mutations that abolish this moiety (A, D, or E) would thus prevent efficient sorting/trafficking of TGN38 out of the endosome, resulting in increased trafficking of TGN38 along a lysosomal pathway. If this were true, one might expect that a T at position 331 would have little effect on the endocytic trafficking of TGN38, provided that the hydroxyl moiety did not significantly alter the secondary structure of the cytosolic domain. To test this hypothesis, we expressed the S331T construct transiently in Cos-7 cells and used the antibody uptake assay described above to assess the ability of the cells to endocytose and localize TGN38 to the TGN. As shown in Figure 10C, the majority of S331T was correctly routed from the cell surface to a juxtanuclear structure (asterisk) identified as the TGN by Brefeldin A treatment (our unpublished observation). Vesicular structures were observed in cells expressing S331T (arrows). However, these vesicles were not sen-

Figure 8. Internalization of wild-type TGN38, S331A, and S331D in the absence or presence of PI3K inhibitor. After growth on glass coverslips and induction to comparable levels with cadmium chloride, monoclonal antibody to TGN38 (2F7.1) was added to the tissue culture medium of cells expressing wild-type TGN38 (A and B), S331A (C and D), and S331D (E and F). Antibody uptake was allowed to proceed to equilibrium at 37°C for 2 h. During the final 30 min of uptake, cells were incubated in the absence (A, C, and E) or presence (B, D, and F) of the PI3K inhibitor LY294002. Fixed cells were incubated with antibody to the endogenous monkey orthologue (P12). Secondary antibodies used were: FITC-conjugated anti-mouse Ig, to detect endocytosed TGN38 antibody, and Texas Red-conjugated anti-rabbit Ig, to detect antibody to the endogenous monkey orthologue. Areas of secondary antibody colocalization are pseudocolored yellow. T, TGN. Arrows, internalized 2F7.1; arrowheads, swollen late endosomes containing internalized 2F7.1.

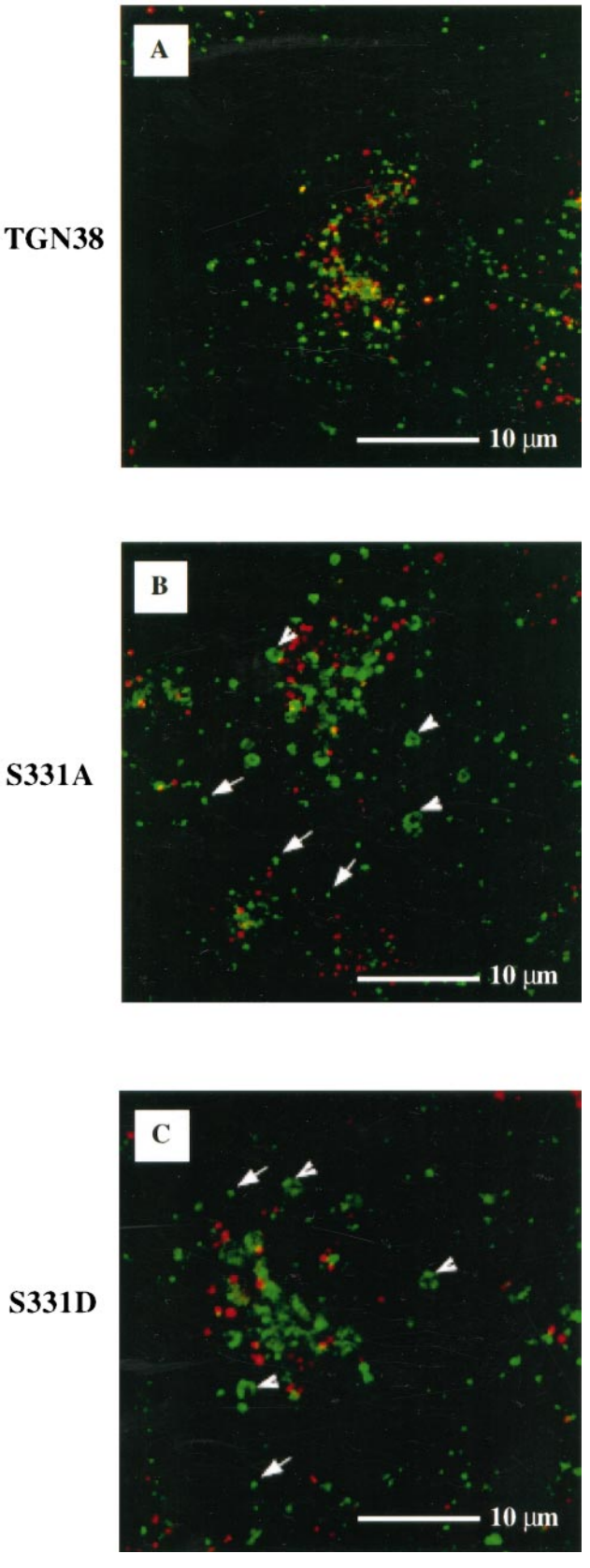

sitive to LY294002 (Figure 10D) and are thus likely to be early endocytic structures, which are also observed in cells transiently transfected with wild-type TGN38 (Figure 10A, arrows).

Molecular Modeling of the Cytosolic Tail of TGN38

To investigate the potential impact of mutations at position 331 on the secondary structure of the cytosolic domain, molecular modeling was performed. Previous two-dimensional nuclear magnetic resonance studies have shown that the SXYQRL motif lies within an α-helix (Wilde *et al.*, 1994). Accordingly, the cytosolic domain of TGN38 was modeled as an α-helix, with substitutions of T, A, D, or E at position 331, as shown in Figure 11. The side-chain torsions presented were chosen based on the results of previous analysis (McGregor *et al.*, 1987) of high-resolution structures from a relational database of protein sequence and structure developed jointly at the Department of Crystallography, Birbeck College, London, and Leeds University, Leeds, England. Such assessment revealed that the most popular rotational angle (C_1) for the side-chain residues, T, D, and E, within an α-helix is the g^+ rotamer, in which the first carbon of the side chain (C_β) is rotated 300° relative to the C_α carbon of the polypeptide backbone (McGregor *et al.*, 1987). When the cytosolic domain of TGN38 is modeled with residues at position 331 in the g^+ C_1 conformation, none of the side chains appears likely to disrupt the ability of the cytosolic domain to maintain an α-helical structure. In addition, the hydroxyl group of a serine or threonine residue at position 331 points away from the helical axis, which would allow it to interact with another hydrogen-bond acceptor, although such access to the threonine hydroxyl group may be somewhat restricted due to the extra methyl group compared with serine.

DISCUSSION

Previous studies from two research groups have identified the tetrapeptide sequence YQRL within the cytosolic domain of TGN38 as being sufficient for internalization and delivery of reporter proteins to the

Figure 9. Antibody uptake after a GPN-induced lysosomal block. Cells expressing wild-type TGN38 (A), S331A (B), or S331D (C) were preincubated for 10 min in the presence of 200 μM GPN to induce swollen, disfunctional lysosomal vacuoles (arrowheads). 2F7.1 ascites was then added to the tissue culture medium at a dilution of 1:400 in the continued presence of GPN. Concomitantly, Texas Red-conjugated transferrin was added at 10 μg/ml to label endosomal compartments. Cells were then incubated for 25 min at 37°C and processed for immunofluorescence using FITC-conjugated anti-mouse Ig to detect endocytosed 2F7.1. Arrows, nonswollen transport vesicles.

TGN (Bos *et al.*, 1993; Humphrey *et al.*, 1993). A third group further implicated an upstream serine residue (corresponding to S331 in wild-type TGN38) as being an important part of the localization motif (Wong and Hong, 1993). However, the hypothesis that S331 plays a role in localization of TGN38 to the TGN was based on results using chimeric constructs and has never been verified within the context of TGN38 itself. Furthermore, the nature of the role played by S331 in the localization of TGN38 has not been addressed. In this paper we have examined the function of S331 in the context of full-length TGN38. The results demonstrate that S331 is indeed important for the intracellular routing of TGN38 and reveal the presence of a critical signal-mediated TGN38 sorting or trafficking step at the level of the endosome.

Mutation of S331 to A or D Leads to an Increase of TGN38 at the Cell Surface

Substitution of A or D at S331 results in a significant (15- to 20-fold) increase of TGN38 at the cell surface, with slightly more S331D detectable at the cell surface than S331A. Stephens *et al.* (1997, and our unpublished observations) have found that mutation of S331 to either A or D decreases the affinity of the cytosolic tail of TGN38 for the μ2 subunit of the AP2 adaptor complex, which is involved in clathrin-mediated endocytosis of specific integral membrane proteins from the cell surface. Decreased affinity for this subunit, and the consequent decrease in clathrin-mediated endocytosis of the protein, would be predicted to lead to enhanced cell surface expression of S331 point mutants and is consistent with the observations presented here. Alternatively, an increase in the rate at which S331A and S331D are delivered from the TGN to the cell surface could also account for the observed increase in cell surface expression.

Elevated surface expression of the S331 mutants is consistent with the results of chimeric studies conducted by Wong and Hong (1993), which show an accumulation of the reporter protein glycophorin A at the cell surface when the S of the SXYQRL motif is mutated to A. It is notable, however, that the amount of cell surface expression observed by Wong and Hong using chimeric constructs containing the S-to-A mutation was significantly more pronounced than that observed here. The efficiency of motifs such as SXYQRL is likely to vary according to the local environment in which they are placed. When mutations are introduced into the SXYQRL motif (e.g., S to A), they may have a more marked effect when expressed in the context of a reporter protein than when presented in the context of full-length TGN38, which is known to have a second localization motif in its transmembrane domain. Thus, our findings further underscore the value of studying localization motifs in their native context.

Marks *et al.* (1996) have demonstrated that overexpression of proteins containing YXXΦ motifs (where Φ represents any residue with a bulky hydrophobic side chain) results in their appearance at the cell surface due to saturation of components of the clathrin-mediated endocytosis machinery. However, the phenomenon of overexpression cannot account for the increased surface expression of the TGN38 tail mutants observed here, since mature forms of both the S331 mutants and the wild-type protein are expressed to similar levels, but only the S331 mutants are detected in significant amounts at the cell surface by biotinylation and indirect immunofluorescence. Even when expression levels of wild-type TGN38 are increased 10-fold, no change in the percentage of TGN38 at the cell surface can be detected (Reaves and Banting, 1994, and our unpublished observations).

Serine 331 Plays a Role in Correct Endocytic Trafficking of TGN38

Using antibody uptake experiments to examine the ability of transfected cells to internalize TGN38 and localize it to the TGN, we have shown that mutation of S331 to A, D, or E increases the appearance of the mutant proteins in late endosomes and/or lysosomes. The kinetics of appearance of internalized S331A and S331D in compartments sensitive to GPN are rapid (within 20–25 min), indicating that misrouting of the S331 mutants to the lysosomes occurs along the endocytic pathway, rather than along an exocytic pathway after exit from the TGN. Consistent with increased trafficking along an endocytic lysosomal pathway, S331A and S331D show elevated rates of degradation in the absence of protein synthesis. Furthermore, the enhanced degradation of S331D can be diminished by incubation of the cells with lysosomal inhibitors. Taken together, the evidence presented indicates that substitution of either A or D for the S331 in the cytosolic domain of TGN38 decreases its retrieval to the TGN and concomitantly increases its passage through a lysosomal pathway. Because the dynamic nature of endocytic compartments makes it difficult to define and distinguish between late endosomes and lysosomes, and since the precise itinerary of TGN38 along the endocytic pathway is not known, these data can be interpreted in two ways: 1) it may be that the late endosome is an obligate, but highly transient, intermediate in the trafficking of TGN38 from the cell surface to the TGN. Mutation of S331 to A, D, or E would delay exit of TGN38 from the late endosome, resulting in degradation of the lingering protein, either in the late endosome itself or in the mature lysosome; 2) alternatively, TGN38 may be routed directly from the early endosome to the TGN, normally bypassing the

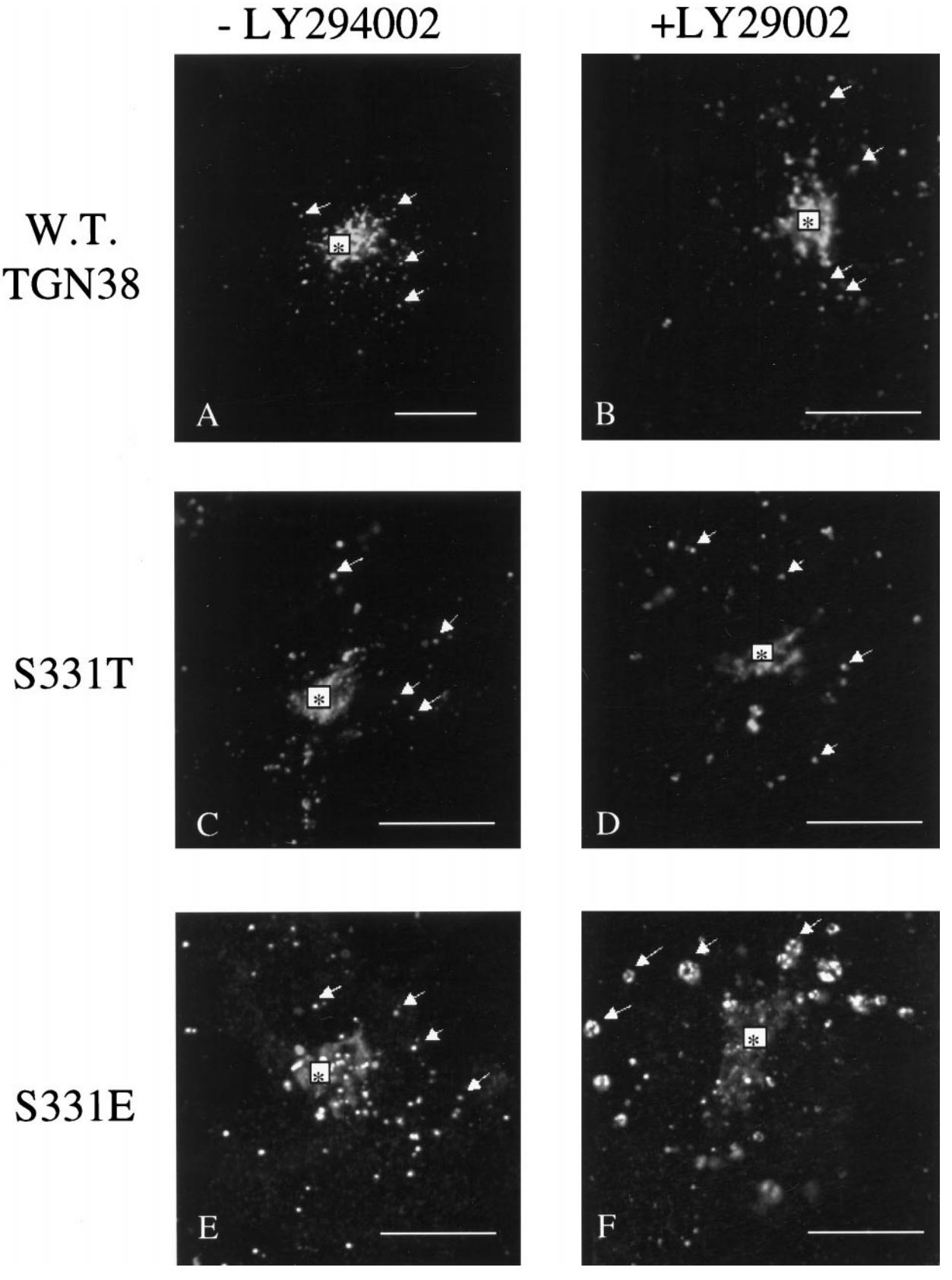

Figure 10.

late endosomal/lysosomal pathway, except when accessibility of S331 is blocked. In either case, the data suggest that S331 is a critical element of a TGN targeting signal that is decoded in the endosome (either early or late), or that S331 is important in establishing proper presentation of the TGN targeting signal to endosomal sorting machinery. Failure to exit the endosome efficiently results in enhanced degradation of TGN38. This finding sheds light on the observation of Wong and Hong (1993) that the amount of reporter protein in the TGN was decreased when S was mutated to A, since increased routing of the reporter protein along a degradative pathway could be expected to produce just such a distribution.

A Free Hydroxyl Moiety at Position 331 Is Critical for Efficient Endocytic Trafficking of TGN38 to the TGN

The hypothesis that S331 in the cytosolic domain of TGN38 is important for correct trafficking of TGN38 from the endosome to the TGN implies the existence of trafficking or sorting machinery capable of recognizing the TGN-targeting motif at the level of the endosome. Substitution of A, D, or E at position 331 leads to an increased abundance of TGN38 in lysosomal compartments. The observation that both S331D and S331E behave similarly to S331A, while S331T behaves similarly to wild-type TGN38, strongly suggests that 1) the hydroxyl group of S331 participates directly in interactions with trafficking or sorting machinery, and that substitution of A, D, or E for S331 prevents these interactions; or 2) that S331 is responsible for proper presentation of the TGN targeting motif to endocytic sorting machinery. In the latter case, the hydroxyl group would presumably be the most important element of the side chain for enabling correct presentation of the targeting motif, since a threonine at position 331 can also fulfill this function, whereas side chains lacking a hydrogen bond donor cannot.

Alternatively, it is possible that mutations at S331 alter the conformation of TGN38 in such a way as to promote aggregation of TGN38. Aggregation of proteins has long been associated with routing along a lysosomal pathway (Mellman and Plunter, 1984; Marsh *et al.*, 1995). However, this interpretation of the data is unlikely to be correct, given the observation that substitution of an alanine residue at position 331 leads to lysosomal routing of TGN38, whereas substitution of the more bulky threonine residue does not. As illustrated in Figure 11, alanine is the least disruptive possible substitution for a serine residue, since the only difference between the two side chains is the replacement of the serine hydroxyl group with a hydrogen ($-CH_2OH$ becomes $-CH_3$). This subtle modification is unlikely to lead to the types of gross morphological alterations in the structure of TGN38 that would be necessary to promote aggregation. Indeed, molecular modeling studies (Figure 11) indicate that none of the mutations used in this study is likely to affect significantly the secondary structure of the TGN38 cytosolic domain.

Possible Mechanisms for Routing of S331 Mutants to the Lysosome

One possible interpretation of the data presented here is that the presence of a serine residue at position 331 in the cytosolic tail of TGN38 minimizes lysosomal routing of TGN38 by optimizing the efficiency with which TGN38 exits the endosome en route to the TGN. A similar observation has been made in the case of the cation-dependent mannose-6-phosphate receptor, in which the cytosolic sequence CRSKPR, upstream of the tyrosine-based internalization motif, is required to prevent trafficking to the lysosomes (Rohrer *et al.*, 1995). The authors suggest that the simplest mechanism by which such a signal could act would be to mediate the sequestration of proteins into endosomal subdomains from which TGN-directed vesicles are derived. Thus, S331 could act in a similar way to promote incorporation of TGN38 into TGN-directed vesicles. Elements from two different classes of vesicle coat (COP1 subunits and clathrin-adaptor complexes) have been observed on early endosomes (Whitney *et al.*, 1995; Aniento *et al.*, 1996; Stoorvogel *et al.*, 1996), although whether they play a role in sorting from this compartment is not yet known. In a manner analogous to the situation with the AP2 adaptor complex (Stephens *et al.*, 1997), S331 could be important for optimizing the affinity of TGN38 for elements of these or other as yet uncharacterized coat complexes functioning at the level of the endosome, and could thereby enhance the ability of TGN38 to be sequestered into TGN-directed vesicles. Experiments aimed at determining whether S331 is involved in binding of TGN38 to elements of putative endosomal coat complexes should prove informative. Thus, S331 could act as a molecular switch to allow TGN38 to enter either TGN

Figure 10 (facing page). Internalization of transiently expressed wild-type TGN38, S331T, and S331E in the absence or presence of PI3K inhibitor. Cos-7 cells were transiently transfected with wild-type TGN38, S331T, or S331E. Monoclonal antibody to TGN38 (2F7.1) was added to the tissue culture medium, and antibody uptake was allowed to occur for 2 h as described in the legend to Figure 8. During the final 30 min of uptake, cells were incubated in the absence (A, C, and E) or presence (B, D, and F) of the PI3K inhibitor LY294002 to identify late endosomes. Cells were fixed and processed for immunofluorescence microscopy as described in the legend to Figure 8. Regardless of the construct expressed, internalized 2F7.1 appeared in numerous peripheral vesicular structures (arrows). Only in cells expressing S331E did internalized 2F7.1 accumulate in swollen vesicular structures in response to LY294002 treatment (F, arrows). Asterisks, TGN. Bars, 10 μm.

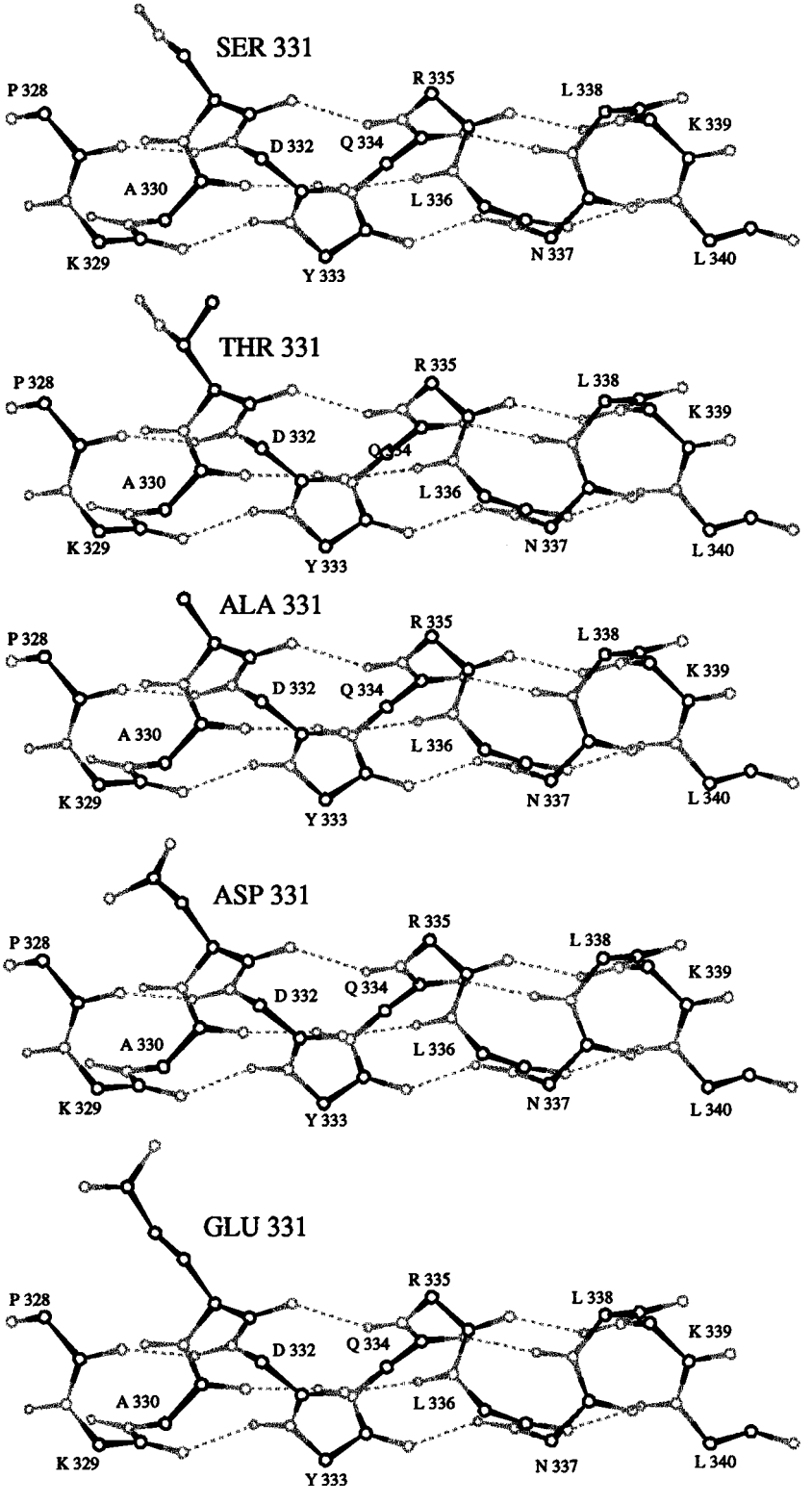

Figure 11. A representation of the heavy atoms and polar hydrogens of the backbone of the cytosolic domain of TGN38, including the side-chain atoms of residue 331. The structures are ordered according to the residue at position 331: S, T, A, D, and E. All side chains are shown in the C_1 g^+ conformation. Carbon atoms are black; all others are gray.

or lysosomally directed pathways: TGN38 with an accessible S331 hydroxyl would be routed to the TGN, while blocking of S331 either by posttranslational modification or by interaction with other proteins, would result in routing of TGN38 to the lysosome.

Concluding Remarks

The results presented in this paper demonstrate that S331 is essential for efficient localization of TGN38 along its endocytic pathway, and therefore the minimum TGN localization motif can be defined accurately as SXYQRL. Although the tetrapeptide YQRL motif alone is sufficient for TGN localization in some chimeric constructs, S331 is clearly required for optimum efficiency of the motif within TGN38 itself. In addition, the data extend current knowledge about the trafficking of TGN38 along the endocytic pathway, by revealing the presence of a distinct signal-mediated transport step at the level of the endosome. Thus, transport of at least some TGN-localized proteins from the endosome to the TGN occurs by active sorting through the recognition of a discrete signal, rather than by a default bulk-flow mechanism. The data we present demonstrate the importance of studying the role(s) of trafficking motifs under conditions that reflect, as faithfully as possible, those under which the endogenous motifs operate. Similar studies on trafficking motifs in other integral membrane proteins may well aid in unraveling the complexities of the finely balanced mechanisms that ensure the fidelity and efficiency of membrane trafficking events in eukaryotic cells.

ACKNOWLEDGMENTS

We gratefully acknowledge Dr. S. Ponnambalam for generously providing antibody to primate TGN46, and Dr. R.B. Sessions for the modeling studies presented as Figure 11. We also thank C. Crump, Dr. S. Kupzig, and Dr. D. Stephens for critical reading of the manuscript, the Medical Research Council for providing an Infrastructure Award (G4500006) to establish the School of Medical Sciences Cell Imaging Facility, and Dr. Mark Jepson for his assistance with confocal image processing. This work was supported by a grant from the Wellcome Trust.

REFERENCES

Aniento, F., Gu, F., Parton R.G., and Gruenberg, J. (1996). An endosomal β-COP is involved in the pH-dependent formation of transport vesicles destined for late endosomes. J. Cell Biol. *133*, 29–41.

Banting, G., and Ponnambalam, S. (1997). TGN38 and its orthologues: roles in post-TGN vesicle formation and maintenance of TGN morphology. Biochim. Biophys. Acta Mol. Cell Res. *1355*, 209–217.

Berg, T.O., Stromhaug, P.E., Lovdal, T., Seglen, P.O., and Berg, T. (1994). Use of glycyl-L-phenylalanine 2-naphthylamide, a lysosome-disrupting cathepsin C substrate, to distinguish between lysosomes and prelysosomal endocytic vacuoles. Biochem. J. *300*, 229–236.

Bos, K., Wraight, C., and Stanley, K. (1993). TGN38 is maintained in the *trans*-Golgi network by a tyrosine-containing motif in the cytoplasmic domain. EMBO J. *12*, 2219–2228.

Casanova, J.E., Breitfeld, P.P., Rosa, S.A., and Mostov, K.E. (1990). Phosphorylation of the polymeric immunoglobulin receptor is required for its efficient transcytosis. Science *248*, 742–745.

Clague, M.J., Thorpe, C., and Jones, A.T. (1995). Phosphatidylinositol 3-kinase regulation of fluid phase endocytosis. FEBS Lett. *367*, 272–274.

Dittie, A.S., Thomas, L., Thomas, G., and Tooze, S.A. (1997). Interaction of furin in immature secretory granules from neuroendocrine cells with the AP-1 adaptor complex is modulated by casein kinase II phosphorylation. EMBO J. *16*, 4859–4870.

Horn, M., and Banting, G. (1994). Okadaic acid treatment leads to a fragmentation of the *trans*-Golgi network and an increase in expression of TGN38 at the cell surface. Biochem. J. *301*, 69–73.

Humphrey, J.S., Peters, P.J., Yuan, L.C., and Bonifacino, J.S. (1993). Localization of TGN38 to the *trans*-Golgi network: involvement of a cytoplasmic tyrosine-containing sequence. J. Cell Biol. *120*, 1123–1135.

Johnson, A.O., Ghosh, R.N., Dunn, K.W., Garippa, R., Park, J., Mayor, S., Maxfield, F.R., and McGraw, T.E. (1996). Transferrin receptor containing the SDYQRL motif of TGN38 causes a reorganization of the recycling compartment but is not targeted to the TGN. J. Cell Biol. *135*, 1749–1762.

Jones, B.G., Thomas, L., Molloy, S.S., Thulin, C.D., Fry, M.D., Walsh, K.A., and Thomas, G. (1995). Intracellular trafficking of furin is modulated by the phosphorylation state of a casein kinase II site in its cytoplasmic tail. EMBO J. *14*, 5869–5883.

Jones, S.M., Crosby, J.R., Salamero, J., and Howell, K.E. (1993). A cytosolic complex of p62 and rab6 associates with TGN38/41 and is involved in budding of exocytic vesicles from the *trans*-Golgi network. J. Cell Biol. *122*, 775–788.

Korner, C., Herzog, A., Weber, B., Rosorius, O., Hemer, F., Schmidt, B., and Braulke, T. (1994). In vitro phosphorylation of the 46-kDa mannose 6-phosphate receptor by casein kinase II. Structural requirements for efficient phosphorylation. J. Biol. Chem. *269*, 16529–16532.

Kornfeld, S. (1992). Structure and function of the mannose 6-phosphate/insulin-like growth factor II receptors. Annu. Rev. Biochem. *61*, 307–330.

Kortnenjann, M., Thomae, O., and Shaw, P.E. (1994). Inhibition of v-raf-dependent c-fos expression and transformation by a kinase-defective mutant of the mitogen-activated protein kinase Erk2. Mol. Cell. Biol. *14*, 4815–4824.

Lippincott-Schwartz, J., Donaldson, J.G., Schweizer, A., Berger, E.G., Hauri, H.P., Yuan, L.C., and Klausner, R.D. (1990). Microtubule-dependent retrograde transport of proteins into the ER in the presence of brefeldin-A suggests an ER recycling pathway. Cell *60*, 821–836.

Lippincott-Schwartz, J., Yuan, L., Tipper, C., Amherdt, M., Orci, L., and Klausner, R.D. (1991). Brefeldin-A's effects on endosomes, lysosomes, and the TGN suggest a general mechanism for regulating organelle structure and membrane traffic. Cell *67*, 601–616.

Luzio, J.P., Brake, B., Banting, G., Howell, K.E., Braghetta, P., and Stanley, K.K. (1990). Identification, sequencing and expression of an integral membrane protein of the *trans*-Golgi network (TGN38). Biochem. J. *270*, 97–102.

Marks, M.S., Ohno, H., Kirchhausen, T., and Bonifacino, J.S. (1997). Protein sorting by tyrosine-based signals: adapting to the Ys and wherefores. Trends Cell Biol. *7*, 124–128.

Marks, M.S., Woodruff, L., Ohno, H., and Bonifacino, J.S. (1996). Protein targeting by tyrosine- and di-leucine-based signals: evidence for distinct saturable components. J. Cell Biol. *135*, 341–354.

Marsh, E.W., Leopold, P.L., Jones, N.L., and Maxfield, F.R. (1995). Oligomerized transferrin receptors are selectively retained by a lumenal sorting signal in a long-lived endocytic compartment. J. Cell Biol. *129*, 1509–1522.

Mauxion, F., Le Borgne, R., MunierLehmann, H., and Hoflack, B. (1996). A casein kinase II phosphorylation site in the cytoplasmic domain of the cation-dependent mannose 6-phosphate receptor determines the high affinity interaction of the AP-1 Golgi assembly proteins with membranes. J. Biol. Chem. *271*, 2171–2178.

McGregor, M.J., Islam, S.A., and Sternberg, M.J. (1987). Analysis of the relationship between side-chain conformation and secondary structure in globular proteins. J. Mol. Biol. *198*, 295–310.

Mellman, I., and Plunter, H. (1984). Internalization and degradation of macrophage Fc receptors bound to polyvalent immune complex. J. Cell Biol. *98*, 1170–1177.

Mostov, K.E. (1995). Regulation of protein traffic in polarized epithelial cells. Histol. Histopathol. *10*, 423–431.

Ohno, H., Fournier, M.C., Poy, G., and Bonifacino, J.S. (1996). Structural determination of interaction of tyrosine-based sorting signals with the adaptor medium chains. J. Biol. Chem. *271*, 29009–29015.

Ohno, H., Stewart, J., Fournier, M.C., Bosshart, H., Rhee, I., Miyatake, S., Saito, T., Gallusser, A., Kirchhausen, T., and Bonifacino, J.S. (1995). Interaction of tyrosine-based sorting signals with clathrin-associated proteins. Science *269*, 1872–1875.

Okamoto, C.T., Song, W., Bomsel, M., and Mostov, K.E. (1994). Rapid internalization of the polymeric immunoglobulin receptor requires phosphorylated serine 726. J. Biol. Chem. *269*, 15676–15682.

Prescott, A.R., Lucocq, J.M., James, J., Lister, J.M., and Ponnambalam, S. (1997). Distinct compartmentalization of TGN46 and beta1,4-galactosyltransferase in HeLa cells. Eur. J. Cell Biol. *72*, 238–246.

Reaves, B., and Banting, G. (1992). Perturbation of the morphology of the trans-Golgi network following Brefeldin A treatment: redistribution of a TGN-specific integral membrane protein, TGN38. J. Cell Biol. *116*, 85–94.

Reaves, B., and Banting, G. (1994). Overexpression of TGN38/41 leads to mislocalisation of γ-adaptin. FEBS Lett. *351*, 448–456.

Reaves, B., Horn, M., and Banting, G. (1993). TGN38/41 recycles between the cell surface and the TGN: brefeldin A affects its rate of return to the TGN. Mol. Biol. Cell *4*, 93–105.

Reaves, B.J., Banting, G., and Luzio, J.P. (1998). Lumenal and transmembrane domains play a role in sorting type I membrane proteins on endocytic pathways. Mol. Biol. Cell *9*, 1107–1122.

Reaves, B.J., Bright, N.A., Mullock, B.M., and Luzio, J.P. (1996). The effect of wortmannin on the localisation of lysosomal type 1 integral membrane glycoproteins suggests a role for phosphoinositide 3-kinase activity in regulating membrane traffic late in the endocytic pathway. J. Cell Sci. *109*, 749–762.

Rohrer, J., Schweizer, A., Johnson, K.F., and Kornfeld, S. (1995). A determinant in the cytoplasmic tail of the cation-dependent mannose-6-phosphate receptor prevents trafficking to lysosomes. J. Cell Biol. *130*, 1297–1306.

Sambrook, J., Fritsch, E.F., and Maniatis, T. (1989). Molecular Cloning: A Laboratory Manual. Cold Spring Harbor, NY: Cold Spring Harbor Laboratory Press.

Sandoval, I.V., and Bakke, O. (1994). Targeting of membrane proteins to endosomes and lysosomes. Trends Cell Biol. *4*, 292–297.

Schweizer, A., Kornfeld, S., and Rohrer, J. (1996). Cysteine-34 of the cytoplasmic tail of the cation-dependent mannose 6-phosphate receptor is reversibly palmitoylated and required for normal trafficking and lysosomal sorting. J. Cell Biol. *132*, 577–588.

Shepherd, P.R., Reaves, B.J., and Davidson, H.W. (1996). Phosphoinositide 3-kinases and membrane traffic. Trends Cell Biol. *6*, 92–97.

Shpetner, H., Joly, M., Hartley, D., and Corvera, S. (1996). Potential sites of PI-3 kinase function in the endocytic pathway revealed by the PI-3 kinase inhibitor, wortmannin. J. Cell Biol. *132*, 595–605.

Song, W., Apodaca, G., and Mostov, K. (1994). Transcytosis of the polymeric immunoglobulin receptor is regulated in multiple intracellular compartments. J. Biol. Chem. *269*, 29474–29480.

Stephens, D.J., Crump, C.M., Clarke, A.R., and Banting, G. (1997). Serine 331 and tyrosine 333 are both involved in the interaction between the cytosolic domain of TGN38 and the μ2 subunit of the AP2 clathrin adaptor complex. J. Biol. Chem. *272*, 14104–14109.

Stoorvogel, W., Oorschot, V., and Geuze, H.J. (1996). A novel class of clathrin-coated vesicles budding from endosomes. J. Cell Biol. *132*, 21–33.

Takahashi, S., Nakagawa, T., Banno, T., Watanabe, T., Murakami, K., and Nakayama, K. (1995). Localization of furin to the trans-Golgi network and recycling from the cell surface involves Ser and Tyr residues within the cytoplasmic domain. J. Biol. Chem. *270*, 28397–28401.

Thorsness, P.E., and Koshland, D.E.J. (1987). Inactivation of isocitrate dehydrogenase by phosphorylation is mediated by the negative charge of the phosphate. J. Biol. Chem. *262*, 10422–10425.

Trowbridge, I.S., Collawn, J.F., and Hopkins, C.R. (1993). Signal-dependent membrane protein trafficking in the endocytic pathway. Annu. Rev. Cell Biol. *9*, 129–161.

Whitney, J.A., Gomez, M., Sheff, D., Kreis, T.E., and Mellman, I. (1995). Cytoplasmic coat proteins involved in endosome function. Cell *83*, 703–713.

Wilde, A., Dempsey, C., and Banting, G. (1994). The tyrosine-containing internalisation motif in the cytoplasmic domain of TGN38/41 lies within a nascent helix. J. Biol. Chem. *269*, 7131–7136.

Wilde, A., Reaves, B., and Banting, G. (1992). Epitope mapping of two isoforms of a trans Golgi network specific integral membrane protein TGN38/41. FEBS Lett. *313*, 235–238.

Wong, S.H., and Hong, W. (1993). The SXYQRL sequence in the cytoplasmic domain of TGN38 plays a major role in trans-Golgi network localization. J. Biol. Chem. *268*, 22853–22862.

Yuan, L., Barriocanal, J.G., Bonifacino, J.S., and Sandoval, I.V. (1987). Two integral membrane proteins located in the *cis*-middle and *trans*-part of the Golgi system acquire sialylated N-linked carbohydrates and display different turnovers and sensitivity to cAMP-dependent phosphorylation. J. Cell Biol. *105*, 215–227.

ZehaviFeferman, R., Burgess, J.W., and Stanley, K.K. (1995). Control of p62 binding to TGN38/41 by phosphorylation. FEBS Lett. *368*, 122–124.